Growth of Mushroom-like Carbon Nanotubes and Nanodiamond Directly on Hydroxyapatite via MPECVD

El-Shazly M. Duraia*[1,2], Gary W. Beall[2,3]

[1]Suez Canal University, Faculty of Science, Physics Department, Ismailia Egypt.
[2]Texas State University-San Marcos, Department of Chemistry and Biochemistry, 601 University Dr., San Marcos, TX 78666, USA
[3]Physics Department, Faculty of Science, King Abdulaziz University, Jeddah 21589, Saudi Arabia
*duraia_physics@yahoo.com

Abstract

Mushroom-like carbon nanotubes (CNTs) and spherical nanodiamond, 3 nm in diameter, have been successfully grown directly on hydroxyapatite (HA) via microwave plasma enhanced chemical vapor deposition (MPECVD) for the first time. The diameter of the CNTs was found to be not uniform while its length was about 500 nm. The HA partially transformed to the β-tricalcium phosphate through dehydroxylation. In all samples, the intensity of the G-band was higher than that of the D-band, which indicates that the grown CNTs have good quality. Water vapor that comes out during the dehydroxylation removes the amorphous carbon and improves the quality of the produced CNTs. Raman analysis showed that there is a shift by 5cm^{-1} from first order peak for the bulk diamond due to the phonon confinement.

Keywords

CNTs; Nanodiamond; Hydroxyapatite; MPECVD; Raman Spectroscopy

Introduction

Despite of its excellent biocompatibility with soft tissues, Hydroxyapatite (HA: $Ca_{10}(PO_4)_6(OH)_2$) ceramics has low fracture strength, which made it inappropriate for many applications and limited its use mainly to conditions of low load-bearing applications. Actually, these drawbacks of the HA can be solved by using composites of metals and hydroxyapatite or calcium phosphates (*Wan* 2007) . To enhance the mechanical properties of the HA, many attempts have been done; such as plasma sprayed HA coatings on metallic implants that were extensively used to improve their biocompatibility (*Christel 1991*). CNTs with its exceptional physical and chemical properties could be a good candidate to improve the physical properties of the HA. In a previous work, CNTs were used as filler to enhance the physical properties of some materials such as polymers or diatomite (*Duraia 2010*). Some authors reported about processing of HA–CNT composite coating for bone implants through laser surface alloying (*Chen 2007*), electrophoretic deposition (EPD) (*Kaya 2008*) and plasma spraying (PS) (*Eliaz 2005; Balani 2007; Balani 2009*). The latter is the common technique used in industry, however, this method has many drawbacks regarding the long term stability of the HA coated implants due to the weak adhesion, non-uniformity and amorphous structure, moreover, it requires a very high temperature. Recently, Rath et al. reported the formation of multiwalled carbon nanotubes (MWCNTs) reinforced hydroxyapatite-chitosan composite coating on Ti metal using EPD technique (*Rath 2012*). The composite HAp-chitosan-MWCNT coating has a better adhesion strength and microhardness than Hap coating. Among all methods used to prepare CNTs, MPECVD method merits many advantages regarding the uniformity of heating and the lower growth temperature over other methods used for CNTs preparations (*Duraia 2010*).

Nano-diamond is of interest owing to its superior mechanical properties, thermal conductivity and electrical and optical properties. It has been proven that nano-diamond is an excellent candidate for many applications electrochemical as biomedical composites. This might be attributed to the fact that nano-diamond combines the characteristics of diamond and those of powders such as large surface area and good chemical activity (*Williams 2011*).

In literature, there are some reports about mixing CNTs with HA, however, there is no reports about growth of carbon nano-materials such as CNTs and nano-diamond directly on the HA. In this work, CNTs

and spherical nano-diamond have been grown directly on HA by using MPECVD.

Experimental

Commercial hydroxyapatite (Sigma-Aldrich) was used as a substrate. About 0.5g of HA has been pressed to form disk of diameter 1cm. Two different methods have been used for the growth of mushroom-like CNTs and nanodiamond, respectively. For the growth of mushroom-like CNTs; thin film, about 5 nm, of nickel catalyst was sputtered on the surface of the substrates by using ion beam evaporation. SEKI AX5200S MPECVD reactor was used for the growth, and more information about this reactor can be found in the references [*Duraia 2010; Duraia 2009*]. The effect of the different MPECVD parameters such as the growth temperature (within the range 500°C -750°C), plasma power (400-700) watt, gas pressure and flow rate were studied. For the growth of the nano-diamond, the substrate was subjected to biased voltage in order to create high nucleation density (from zero to -300V).

Th samples have been investigated by means of scanning electron microscope JEOL JSM-6490LA with resolution (3 nm), which is attached by energy dispersed X-ray spectroscopy EDAX and high resolution transmission electron microscope HRTEM JOEL 1230. Raman spectroscopy was performed by using (NT-MDT, NTEGRA Spectra) with excitation Ar laser 473 nm at room temperature. The x-ray analysis was carried out on a Bruker D-8 diffractometer utilizing Cu Ka radiation. The patterns were scanned from 16 to 105 degrees 2θ at a step size of 0.02 degrees and step time of 3 seconds.

Results And Discussions

Figure 1 depicts the XRD of the HA after the growth of the CNTs. X-ray peaks of the formed phase were matched to the ICDD (JCPDS) standard, α-tricalcium phosphate (09-0348) and β-tricalcium phosphate (03-0690). The substrate temperature for this sample was 700°C which is considered to be lower than the temperature sufficient for the conversion to the β-tricalcium phosphate. However, during the deposition process, microwave plasma adds more heat and increases the temperature of the substrate's upper surface, therefore, the HA-substrate surface is subjected to a temperature sufficient for conversion to the β-tricalcium phosphate. The first step in the thermal decomposition of HA is the dehydroxylation to oxyhydroxyapatite which takes place at about 850-900°C (*Ramesh 2008*).

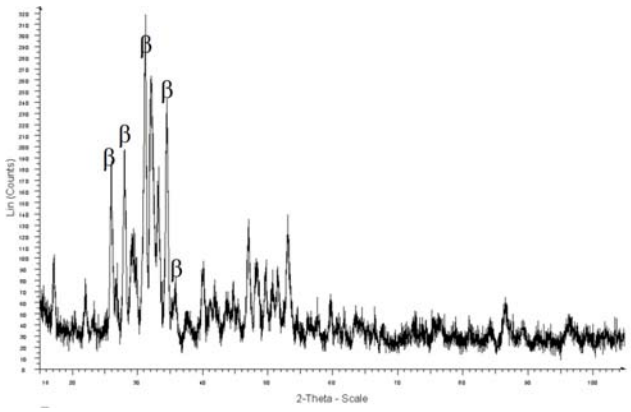

FIG. 1 XRD OF THE HYDROXYAPATITE AFTER GROWTH OF CNTS

Secondary phase formation could be prevented by the water vapor that comes as a product of the dehydroxylation and the thermal decomposition during sintering. The presence of moisture in the sintering atmosphere has slowed down the decomposition rate by preventing the loss of the OH group from the HA matrix. Mayer et al. (*Mayer 2008*) showed that the heat treatment of Mn doped HA at 800°C for 5h is sufficient for partially or almost completely HA to β-TCP transformation. In the present work, the plasma effect is expected to raise the temperature of the HA-substrate surface exposed to higher than 800°C during the deposition time. No conspicuous chemical reaction was recorded between CNT and HA through the spark plasma sintering (*Xu 2009*) which is in accordance with the present findings.

Figure 2 represents the SEM images of CNTs which were grown directly on the HA at different magnifications. CNTs diameters was about 50 nm and not uniformin figure 2d, whereas the length is relatively small about 500 nm, indicating that the aspect ratio is about 10. The growth conditions for this sample were as following, growth temperature 700°C, methane flow rate 5 sccm (standard cubic centimeter per minute), hydrogen 100 sccm, gas pressure 15 torr and the growth time was 10 min. The short CNTs is very important to understand the growth mechanism of the CNTs. Small growth rate of the CNTs can be explained by the low flow rate of methane which implies small amount of hydrocarbon supply (in this case, only 5sccm have been used) resulting in high quality CNTs with lower defects and good crystallinity.

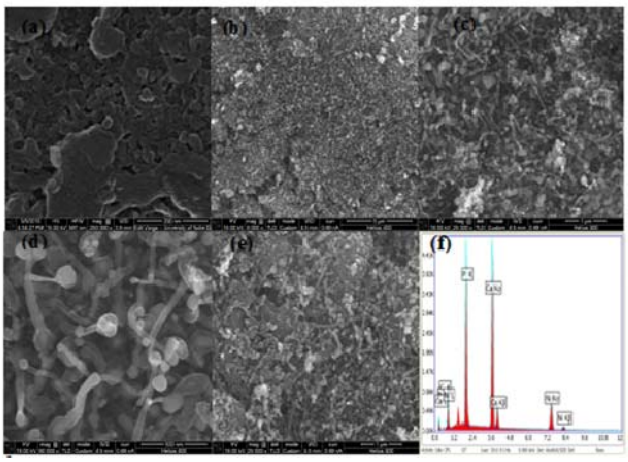

FIG. 2 SEM IMAGES OF HA BEFORE CNTS GROWTH (A), CNTS WHICH WERE GROWN DIRECTLY ON THE HA AT DIFFERENT MAGNIFICATIONS (B-E) AND EDX ANALYSIS (F)

Diameter of the grown CNTs was not uniform. It was noticed that the diameter is large at the bottom and becomes small at the end and it looks like mushroom. Catalyst nanoparticles are found at the top of the CNTs, which indicated that the growth mechanism was via tip-mechanism. Moreover; as it can be noticed from Fig. 2c, 2d and 3c, 3d that there are some needle-like structures found to be from HA as indicated from the EDS analysis. It has been known that HA can form non-equi-axial crystallites of possible rod-like and ribbon-like morphology even under equilibrium growth conditions and ideal stoichiometry (*Silva 2004*). These HA rod-like structures have been developed during the thermal annealing before starting the growth process.

The growth temperature was found to be an important parameter in the growth of the CNTs on HA. When the growth temperature decreased to 500°C as shown in fig.3, the amount of the CNTs was very small. The system was evacuated to $6x10^{-7}$torr and the heater was turned on at 500°C and the pretreatment was done for five minutes at plasma power 700 watt; hydrogen flow rate 90 sccm and the growth process was done at 500 watt for 10 min. An increase of the amount of the CNTs and as well its quality was noticed, when the growth temperature increases to 750 °C. Thus, the ratio IG/ID increased from 1.341 to 1.774 when the growth temperature increased from 500 °C to 750 °C. Simultaneously, the diameter of the CNTs also increased. At high temperature, the small catalyst particle can coalesce together to form bigger particle which will produce CNTs with larger diameter or the catalyst particle may be flat at the higher temperature so it can also produce CNTs with larger diameter (*Duraia 2010*).

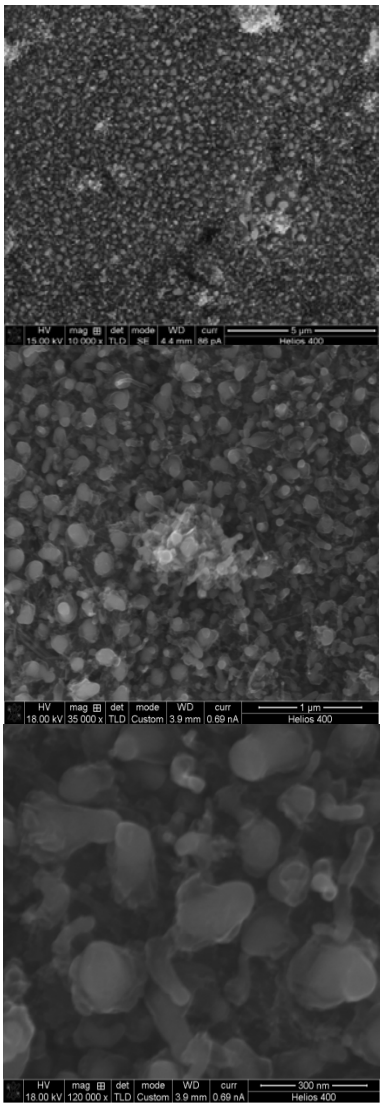

FIG. 3 SEM IMAGES OF CNT ON HA WITHOUT ANNEALING IN VACUUM AT DIFFERENT MAGNIFICATIONS

Raman spectrum of the as-grown samples is represented in figure 4. It is well known that there are two basic peaks characteristic for the carbon nanotubes; the G- band at 1582 cm^{-1} and D-band around 1350 cm^{-1} (*Xu 2009*). Moreover, HA is also Raman active and its spectrum contained bands associated to internal vibrational modes and bands due to the stretching and vibrational modes of the hydroxyl ion. It was observed that the Raman spectrum of the $\nu_1(PO_4)$ band at 959 cm^{-1} was very intense and characteristic for HA. This mode is associated with the totally symmetric $\nu_1(PO_4)$ A1 stretching mode of the free tetrahedral phosphate ion (*Silva 2004*). Before the CNTs growth, Raman spectrum of pure HA contains the intensive $\nu_1(PO_4)$ band at 951 cm^{-1} which is characteristic for HA and weak modes at 430 cm^{-1} and 592 cm^{-1}. After CNTs deposition, Raman spectrum contains three main peaks at 967, 1362 and 1571 cm^{-1}. As the growth temperature increased; the

amount of CNTs increases and the HA peak becomes weak as shown in Fig.4. HA peak in the Raman spectrum of the lower temperature specimen has completely disappeared while at higher temperature the intensity of the peak at 968 cm^{-1} is more conspicuous and another small peak appeared at 1083, which is attributed to $\nu_1(PO_4)$ and $\nu_3(PO_4)$, respectively.

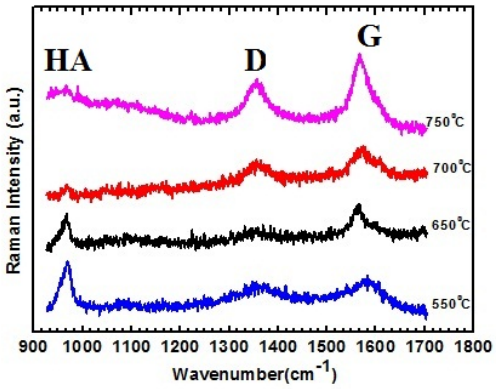

FIG. 4 RAMAN SPECTRA OF CNTS GROWN ON HA AT DIFFERENT GROWTH TEMPERATURES

For all samples, Raman analysis showed the higher intensity of the G-band related to the desirable crystalline of the product and this can be seen from the SEM images, and there is less amorphous carbon. When the same growth conditions and procedure for the substrate preparation have been used for the silicon substrate, higher amounts of amorphous carbon found in the product attached to the carbon nanotube walls. Moreover, the morphology of the CNTs in the case of the silicon substrate was different; while the CNTs in the silicon substrate have uniform diameter and the diameter of the carbon nanotubes in the HA case was not uniform as it has been in the SEM and TEM investigations. So, the central question now is why the CNTs are so clean when HA is used as a substrate. It is well known that water vapor can be during the growth process of the CNTs to control the growth process and remove the amorphous carbon formed during the growth process. This amorphous carbon could poison the catalyst nanoparticle and make it not ready to receive any excess carbon atoms and for this reason the growth process of the CNTs will be ended. Using small amount of the water vapor during the growth process can combust the amorphous carbon by converting it to carbon monoxide gas which can be removed from the reaction chamber by the vacuum system. In the present work, water vapor comes out during the dehydroxylation and the thermal decomposition. Actually, during the growth process, it has been noticed that the plasma color changed most likely due to this water vapor. It is believed that this water vapor played important role in the morphology and structure of the carbon nanotubes in our case.

In order to grow CNTs in our work, nickel nanoparticle has been used to facilitate the growth process. This nanoparticles are toxic and might cause some limitations in the application of the HA in the biological systems. Fortunately, during the investigation under the SEM, it is found that all nickel nanoparticles are covered by carbon. Moreover, the choice of nickel is due to its good catalyst but other nontoxic catalyst could be also used.

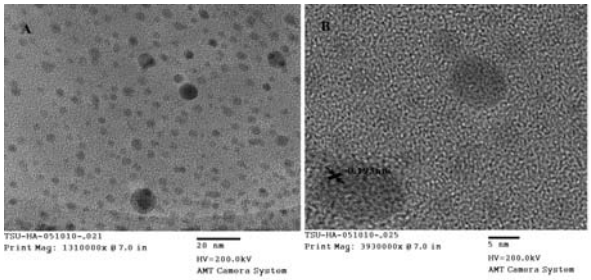

FIG. 5 HRTEM OF CNTS AND NANO-DIAMOND

TEM investigations, Fig.5, showed spherical nano-diamond 3 nm in diameter similar to that in ref. (*Welz 2003*). Through our SEM investigation, it is incapable to see any of these particles because of the low resolution. Typically, nano-diamond is deposited by using gas mixture such as methane and hydrogen plasma at relatively high temperature. High nucleation density is required for the nano-diamond growth; which can be achieved by using mechanical abrasion techniques (scratching), ultrasonic particle treatment (micro-chipping), carbon, carbide and carbide forming interlayers, seeding with diamond nano-particles and bias enhanced nucleation (*Williams 2011*). Here -200V has been used as a bias substrate temperature of 750°C where H_2 and CH_4 flow rate were 300 and10 sccm, respectively. Raman spectroscopy has been done to test the existence of nano-diamond.

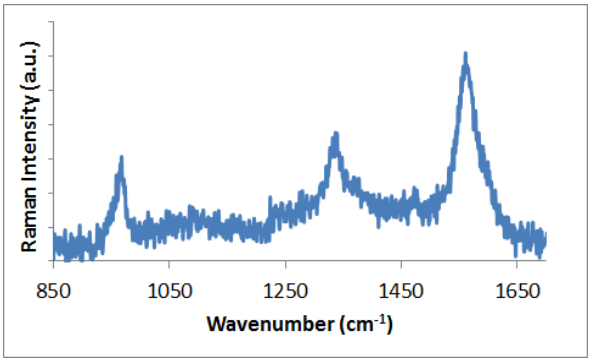

FIG. 6 RAMAN SPECTRUM FOR THE NANO-DIAMOND GROWN OVER HA.

Figure 6 represents the Raman spectrum of the HA coated nano-diamond. There are three major peaks located at 965, 1327 and 1567 cm^{-1}. It is obvious that the first peak is attributed to the HA, the second peak at 1327 is shifted 5 cm^{-1} from first order peak for the bulk diamond. Raman spectrum of the nano-diamond has been studied by many authors (*Prawer 2000*). According to the phonon confinement model:

$$I(\omega) = \int_0^1 \frac{dq \exp\left(-\frac{q^2 l^2}{4}\right) 4\pi q^2}{[\omega - \omega(q)]^2 + (\frac{\Gamma_0}{2})^2}$$

I is the intensity, frequency, q is the phonon wave vector, l is the diameter of the sphere confined phonon where $\omega(q)$ is an approximate one dimensional phonon dispersion curve. As l decreases, the Raman line shape is expected to be asymmetrically broadened and shifts to the lower frequency which is consistent with our results (*Ager 1991*).

The Raman spectrum of CVD diamond can be deconvolved into peaks that can be attributed to diamond and non-diamond components of the film. In the literature (*Prawer 1991; Harris 1996*) many authors have used the ratio $I_{(1332)}/I_{(1500)}$ as a measure of the phase purity of diamond films. For example, the observation of a 1332 cm^{-1} line on a flat background without observable peak in the region 1500–1550 cm^{-1} is often taken as strong evidence for the production of pure diamond virtually without the presence of non-diamond components. This is particularly the case if the measurement is carried out using infrared (IR) excitation, which enhances the Raman sensitivity to the sp2 component of the film. Although, in our case IR is absent from excitation, it is clear that the ratio $I_{(1332)}/I_{(1500)}$ is high, which reflects the higher purity of nanodiamond.

CONCLUSIONS

In summary, mushroom-like CNTs with diameter distribution from 30 to 70 nm and spherical nano-diamond, 3 nm in diameter, have been successively grown directly on the surface of the HA by using MPECVD. Due to the additional plasma heating effect, the HA surface was found to be partially transformed to β-TCP. The structure and the yield of the CNTs could be controlled by the growth temperature as indicated by the SEM and the Raman spectroscopy. Raman analysis showed that the grown CNTs have good quality and the IG/ID ratio is always higher than one. Water vapor that comes out from the HA during the growth process may be responsible for the good quality of the CNTs. Raman study of the nano-diamond showed that there is slightly wide peak centered at 1327 which is shifted 5 cm-1 from first order peak for the bulk diamond due to the phonon confinement. Direct synthesis of CNTs and nano-diamond on HA has vast applications in bio-implementation.

REFERENCES

Ager J., Veirs D., Rosenblatt G., Physical Review B, 43(1991) 6491–6499

Balani K., Anderson R., Laha T, Andara M, Tercero J, Crumpler E, Agarwal A, Biomaterials 28 (2007) 618-624.

Balani K., Lahiri D, Keshri AK, Bakshi SR, Tercero JE, Agarwal A, JOM Journal of the Minerals, Metals and Materials Society 61 (2009) 63–66.

Chen Y., Zhang T. H., Gan C. H., Yu G., Carbon 45 (2007) 998-1004.

Christel Klein P.A.T., Patka P., van der Lubbe H.B.M., Wolke J.G.C., de Groot K., J. Biomed. Mater. Res. 25 (1991) 53–65.

Duraia El-Shazly M. A, Mansurov Z. A, Tokmoldin S. Zh., Physica status solidi, C7 (2010)1222–1226.

Duraia El-Shazly M. A., Burkitbaev M., Mohamedbakr H., Mansurov Z., Beall Gary W., Vacuum 84 (2010) 464–468.

Duraia El-Shazly M., Abdullin Kh.A., Journal of Magnetism and Magnetic Materials 321(2009) L69–L72

Eliaz N., Sridhar M., Mudali U., Raj B., Surf Eng. 21 (2005) 238–242.

Harris J., Weiner M., Prawer S., Kerry N., Journal of Applied Physics 80 [4] (1996) 2187-2194

Kaya C., Singh I., Boccaccini A. R., Advanced Engineering Materials 10 (2008) 131-138.

Mayer I., Cuisinier F. J. G., Gdalya S., Popov I., Journal of Inorganic Biochemistry 102 (2008) 311–317.

Prawer S, Nugent K.W, Jamieson D.N, Orwa J.O, Bursill L.A, Peng J.L, Chemical Physics Letters, Chemical Physics Letters 332 (2000) 93–97

Prawer S., Hoffman A., Stuart S., Manory R., Journal of Applied Physics 69 [9] (1991) 6625 - 6631

Ramesh S., Tana C. Y., Bhadurib S.B., Tengc W.D., Sopyand I., journal of materials processing technology, 206 (2008) 221–230.

Rath P., Singh B., Besra L., Bhattacharjee S., J. Am. Ceram. Soc., 95 [9] (2012)2725–2731

Silva C.C., Sombra A.S.B., Journal of Physics and Chemistry of Solids 65 (2004) 1031–1033.

Wan T., Aoki H., Hikawa J.and Lee J. Bio-Medical Materials and Engineering 17 (2007) 291–297.

Welz, S., Gogotsi, Y., McNallan, M. J., J. Appl. Phys. 93(2003)4207

Williams O.A., Nanocrystalline diamond, Diamond & Related Materials 20 (2011) 621–640

Xu J.L., Khor K.A., Sui J.J., Chen W.N., Materials Science and Engineering C 29 (2009): 44–49.1) 6625 - 6631